

1 **A rapid pharmacogenomic assay to detect *NAT2* polymorphisms and guide isoniazid dosing**
2 **for tuberculosis treatment**

3
4 **Authors:** Renu Verma¹, Sunita Patil¹, Nan Zhang², Flora Martinez Figueira Moreira³, Marize
5 Teixeira Vitorio³, Andrea da Silva Santos³, Ellen Wallace⁴, Devasena Gnanashanmugam⁴, David
6 Persing⁴, Rada Savic², Julio Croda^{5,6}, Jason R. Andrews^{1*}

- 7
8 1. Division of Infectious Diseases and Geographic Medicine, Stanford University School of
9 Medicine, Stanford, CA, USA
10 2. Department of Bioengineering and Therapeutic Sciences, University of California, San
11 Francisco, CA, USA
12 3. Federal University of Grande Dourados, Dourados, Brazil
13 4. Cepheid Inc., Sunnyvale, California, USA
14 5. Postgraduate Program in Infectious and Parasitic Diseases, Federal University of Mato
15 Grosso do Sul, Mato Grosso do Sul, Brazil
16 6. Oswaldo Cruz Foundation Mato Grosso do Sul, Mato Grosso do Sul, Brazil

17
18 **Keywords:** tuberculosis; isoniazid; pharmacogenomic; molecular diagnostic; *NAT2*

19 **Abstract Word Count:** 183

20 **Word Count:** 3,817

21 **Tables:** 3

22 **Figures:** 4

23 **Reference:** 50

24

25 **Correspondence***

26 Jason Andrews, MD

27 Division of Infectious Diseases and Geographic Medicine

28 Biomedical Innovations Building, Room 3458

29 Stanford University School of Medicine

30 Stanford, CA 94305

31 Email: jandr@stanford.edu

32 Phone: +1 650 497 2679

33

34

35 **Abstract**

36 Treatment of tuberculosis involves use of standardized weight-based doses of antibiotics, but
37 there remains a substantial incidence of toxicities, inadequate treatment response, and relapse, in
38 part due to variable drug levels achieved. Single nucleotide polymorphisms (SNPs) in the N-
39 acetyltransferase-2 (*NAT2*) gene explain 88% of interindividual pharmacokinetic variability of
40 isoniazid, one of the two most important antitubercular antibiotics. A major obstacle to
41 implementing pharmacogenomic guided dosing is the lack of a point-of-care assay. We trained
42 an acetylation genotype classification model from a global dataset of 5,738 genomes, which
43 achieved 100% accuracy in out-of-sample prediction on unphased SNPs from 2,823 samples
44 using 5 SNPs. On a clinical dataset of 49 patients with tuberculosis, we found that a 5 SNP assay
45 accurately predicted acetylation ratios and isoniazid clearance. We then developed a cartridge-
46 based molecular assay for the 5 SNPs on the GeneXpert platform, which enabled accurate
47 classification of allele patterns directly from as little as 25 ul of whole blood. An automated
48 pharmacogenomic assay on a platform widely used globally for tuberculosis diagnosis could
49 enable improved dosing of isoniazid, averting toxicities and improving treatment outcomes.

50

51 INTRODUCTION

52 Despite the availability of effective chemotherapeutic regimens for treatment and prevention of
53 tuberculosis, a substantial proportion of patients experience toxicities, fail treatment or develop
54 recurrent disease¹⁻³. Standardized, weight-based dosing of anti-tuberculosis treatment has been
55 the conventional approach to therapy, despite mounting evidence that inter-individual variability
56 in metabolism leads to highly variable drug levels^{4,5}. High drug levels are strongly associated
57 with risk of toxicity, while low drug levels are a determinant of treatment failure, slow response,
58 and emergence of drug resistance. Hepatotoxicity is the most common adverse effect, affecting
59 up to 33% of patients receiving standard four-drug therapy⁶ and leading to regimen changes in
60 up to 10% of patients⁷. This toxicity is associated with increased costs, morbidity, and occasional
61 mortality, particularly among HIV co-infected individuals⁸. Additionally, as many as 3% of new
62 tuberculosis cases experience treatment failure, and between 6-10% relapse within 2 years^{9,10}
63 Pharmacokinetic variability to a single drug is associated with treatment failure and acquired
64 drug resistance^{11,12}. One recent study found that individuals with at least one drug below the
65 recommended AUC threshold had a 14-fold increased risk of poor outcomes.¹³

66 There has been an increasing number of genetic markers identified that predict metabolism and
67 toxicities from various antimicrobials. Isoniazid (INH) is among the most well characterized of
68 these, with 88% of its pharmacokinetic variability explained by mutations in the gene encoding
69 arylamine N-acetyltransferase 2 (NAT2), responsible for acetylation in the liver¹⁴. Individuals
70 can be classified into three phenotypes—rapid, intermediate, and slow acetylators—according to
71 whether they carry polymorphisms on neither, one, or both copies of this gene, respectively.
72 Rapid acetylators typically have the lowest plasma INH concentrations, while slow acetylators

73 have high concentrations. A worldwide population survey on *NAT2* acetylation phenotype
74 reported that more than half of the global population are slow or rapid acetylators¹⁵. Numerous
75 studies have investigated the relationship between acetylation genotype or phenotype and clinical
76 outcomes of tuberculosis treatment. A recent meta-analysis found that rapid acetylators are twice
77 as likely to have microbiological failure and acquired drug resistance¹⁶. Additional meta-analyses
78 have identified a three- to four-fold increased risk of hepatotoxicity among slow acetylators^{17,18}.
79 A recent randomized trial of pharmacogenomic guided dosing for tuberculosis treatment found
80 that, compared with standard dosing, it reduced hepatotoxicity among slow acetylators and
81 increased treatment response at 8 weeks among rapid acetylators¹⁹

82
83 Despite this evidence, pharmacogenomic testing and guided treatment has not entered the
84 mainstream of clinical practice for tuberculosis. Few clinical laboratories perform *NAT2*
85 genotyping, and such testing is not widely available in resource-constrained environments where
86 the majority of tuberculosis burden falls. To address this gap, we developed a prototype *NAT2*
87 pharmacogenomic (*NAT2*-PGx) assay on a commercial, automated PCR platform (GeneXpert)
88 to detect *NAT2* polymorphisms. We further developed an in-house algorithm to predict INH
89 metabolism phenotype from unphased single nucleotide polymorphism (SNP) patterns, derived
90 from globally representative genomic data. We demonstrate that this tool can accurately predict
91 INH clearance rates directly from clinical samples.

92

93

94 **RESULTS**

95 **SNP selection and development of acetylation prediction model**

96 Complete phased data for the seven known polymorphisms (191G>A, rs1801279; 282C>T,
97 rs1041983; 341T>C, rs1801280; 481C>T, rs1799929; 590G>A, rs1799930; 803A>G, rs1208;
98 and 857G>A, rs1799931) altering *NAT2* gene function were available for 8,561 individuals from
99 59 populations. The dataset contains 3,573 (41.7%) individuals with the slow genotype, 3,428
100 (40.0%) individuals with the intermediate genotype, and 1,560 (18.2%) individuals with the
101 rapid genotype (See **Table 1**). The highest proportion of rapid acetylators were in East Asia
102 (40%), and three regions had prevalence of slow acetylator phenotypes over 50% (Central and
103 South Asia, Europe and North Africa).

104 We used these phased allele data to select SNPs for inclusion in an assay measuring unphased
105 SNPs. Using a random forest model trained on two thirds of the data (n=5,738), out-of-sample
106 phenotype prediction accuracy from unphased data on the remaining one third (n=2,823) was
107 100% for models using 7, 6 or 5 SNPs. With 4 SNPs, prediction accuracy was 98.0% (95% CI:
108 97.4-98.5%), and a 3 SNP model had similar performance (98.0%; 95% CI: 97.4-98.4%) (**Table**
109 **2**). However, both of these models performed poorly on data from Sub-Saharan Africa (4 SNP
110 model accuracy: 82.5%, 95% CI: 78.1-86.4%); 3 SNP model accuracy: 81.3%, 95% CI: 76.8-
111 85.3%). Based on these results, we selected the 5 SNP model (191G>A, 282C>T, 341T>C,
112 590G>A and 857G>A) to take forward for clinical validation and diagnostic development.

113

114 **Genotype correlation with isoniazid clearance in patients with tuberculosis**

115

116 We enrolled a cohort of 49 patients with newly diagnosed pulmonary tuberculosis and collected
117 plasma at 1 hour and 8 hours after dose on day 1 and at 1 hour after dose on day 14. To detect
118 five NAT2 polymorphisms identified by our classifier, we performed single-plex PCR assays on
119 49 sputum samples using molecular beacon probes developed in-house (see Methods).
120 Additionally, we used commercial 7-SNP single-plex genotyping assays and compared the
121 results with 5-SNP single-plex PCR to validate the melt curve accuracy. There was 100%
122 concordance in terms of SNP detection between 5-SNP and commercial 7-SNP assays. Of the 49
123 individuals for whom NAT2 genotypes were profiled, ΔT_m ($^{\circ}\text{C}$) between wild-type and mutant
124 alleles for positions 191, 282, 341, 590 and 857 were found to be 4.38, 4.04, 2.40, 3.63 and 3.68
125 respectively. Both mutant and wild type probes had a minimum 2.40°C T_m difference which
126 allowed SNP calling with high accuracy (**Table 3**).

127
128 We further predicted phenotypes from 5-SNP using the algorithm described above as well as a
129 publicly available tool (NAT2Pred)²⁰, which uses 6 SNPs. Among the 49 participants, predicted
130 acetylator types from the 5 SNP assay were: 28 (57%) slow, 16 (33%) intermediate and 5 (10%)
131 rapid. NAT2Pred classified 4 samples as intermediate that were classified as rapid (n=1) or slow
132 (n=3) by the 5 SNP classifier. Among those classified as slow by the 5 SNP classifier and
133 intermediate by NAT2Pred, acetyl-INH to INH ratios at 8 hours were 0.61, 0.38, 0.41, consistent
134 with slow acetylation (median: 0.77, range 0-1.55) rather than intermediate acetylation (median
135 6.67, range 3.32-22.21) and suggesting misclassification by NAT2Pred. The sample classified as
136 intermediate by NAT2Pred and rapid by the 5 SNP classifier had an acetyl-INH to INH ratio of
137 9.8, which fell between the median values, and within both ranges, for intermediate and rapid
138 acetylators (range 8.09 - ∞) (**Supplementary Table-1**). Phenotypes predicted by the 5 SNP

139 classifier were strongly predictive of INH acetylation and clearance (**Figure 1a and 1b**). INH
140 clearance rates were lowest in slow acetylators (median 19.3 L/hr), moderate in intermediate
141 acetylators (median 41.0 L/hr) and highest in fast acetylators (median 46.7 L/hr).

142

143 **Development of an automated pharmacogenomic assay**

144

145 Using the primers and probes sequences validated on FAM-labelled single-plex assays targeting
146 five *NAT2* polymorphisms, we developed a 5-plex multiplex assay using the FleXible Cartridge
147 system on the GeneXpert platform, which enables automated extraction, real-time PCR, melt
148 curve analysis and interpretation in 140 minutes (**Figure 2**). We performed the assay on 20
149 whole blood samples from healthy individuals. Mutant, wild-type and heterozygous alleles were
150 manually called based on peak patterns and T_m values detected in melt curves. Negative
151 derivative transformed melt curves from five *NAT2* gene polymorphisms are shown in **Figure 3**.
152 The genotype data generated on GeneXpert was validated by Sanger sequencing. The assay
153 detected all polymorphisms with 100% accuracy (average SD in T_m across all probes = 0.34°C).
154 The *NAT2* genotypes corresponding to 20 blood samples covered all three categories - mutant,
155 wild-type and heterozygous for five *NAT2* positions except for *NAT2*-191 for which all samples
156 were all wild-type. Among the 20 samples, predicted acetylator types using the 5-SNP classifier
157 were: 8 (40%) slow, 10 (50%) intermediate and 2 (10%) rapid (**Supplementary Table 2a**).

158

159 We used whole blood samples from ten healthy volunteers to assess the analytic performance of
160 the *NAT2*-PGx assay at lower sample volumes. The samples at decreasing volumes (200ul,
161 100ul, 50ul and 25ul) were analyzed until the point where all melt peaks could be accurately

162 detected by GeneXpert. Our assay could accurately detect all melt peaks with as low as 25ul of
163 sample volume. The variability in T_m from five NAT2 probes for sample volumes 200ul-25ul is
164 shown in **Figure 4**. NAT2 polymorphisms were accurately detected at all volumes
165 **(Supplementary Table 2b)**.

166

167 **DISCUSSION**

168

169 Despite availability of effective treatment for drug-sensitive tuberculosis, a substantial
170 proportion of population encounters drug associated toxicity or treatment failure, much of which
171 could be averted through dosing guided by genetic markers of drug metabolism^{21,22}. We
172 previously found that pharmacogenomic guided dosing of isoniazid could be highly cost-
173 effective in low- and middle-income countries²³. A major barrier to its implementation has been
174 the lack of a simple, scalable assay that could be used at points of care where tuberculosis is
175 treated in resource-constrained settings. To address this gap, we used globally representative
176 genomic data to identify patterns of 5 SNPs that enable accurate prediction of isoniazid
177 acetylator phenotype, validating this with pharmacokinetic data of patients receiving tuberculosis
178 treatment. We then developed a prototype automated pharmacogenomic assay on the GeneXpert
179 platform, which is widely available globally but had never been applied to pharmacogenomics.
180 We found that this assay could robustly distinguish wild type, mutant and heterozygous alleles
181 from a range of blood volumes as low as 25 ul, making it suitable for use with venous blood
182 samples or finger-stick blood samples. The assay requires minimal hands-on time for sample
183 preparation, which would facilitate its use in resource-constrained settings.

184

185 An earlier model (“NAT2Pred”) predicted NAT2 acetylation phenotype from unphased genomic
186 data; however, it had moderate error rates in distinguishing intermediate from rapid acetylators²⁴.
187 Moreover, error rates among individuals from Sub-Saharan Africa were 14%, in part due to the
188 exclusion of the G191A (R64Q) SNP, common to the NAT2 *14 allele cluster, which is frequent
189 in Africans and African-Americans, but virtually absent in Caucasian, Indian, and Korean

190 populations²⁵. Indeed, striking ethnic differences in the frequencies of SNPs
191 (<http://snp500cancer.nci.nih.gov>) are responsible for the differences in frequency of rapid,
192 intermediate and slow acetylator *NAT2* alleles or haplotypes and therefore phenotypes^{15, 26, 27}. We
193 trained our SNP classifier with globally representative data, which resulted in the selection and
194 inclusion of the G191A SNP in our model and assay. This is particularly important as Sub-
195 Saharan Africa bears a substantial burden of tuberculosis disease and mortality as well as HIV
196 co-infection, which is independently associated with greater pharmacokinetic variability and
197 tuberculosis treatment toxicity²⁸⁻³¹.

198
199 The association between acetylation polymorphisms and isoniazid metabolism was first
200 demonstrated in 1959, and their importance was well characterized in subsequent decades
201 through phenotypic descriptions³²⁻³⁴. Subsequent genotypic descriptions confirmed that *NAT2*
202 polymorphisms predicted isoniazid early bactericidal activity, and clinical outcomes including
203 hepatotoxicity, relapse and acquisition of drug resistance. Further dosing studies demonstrated
204 that provision of lower doses to slow acetylators and higher doses to rapid acetylators could
205 achieve target concentrations³⁵. One randomized trial of pharmacogenomic-guided dosing of
206 isoniazid during active tuberculosis treatment found that it significantly reduced toxicities
207 (among slow acetylators) and treatment non-response (among rapid acetylators). Taken together,
208 the evidence for pharmacogenomic guided dosing to achieve consistent drug levels and improve
209 clinical outcomes is strong. Automated, easy-to-use assays could enable pharmacogenomic
210 guided isoniazid dosing in resource constrained settings, where a substantial burden of the
211 world's tuberculosis occurs.

212

213 The findings of this study are subject to several limitations. We tested the assays on 49
214 individuals with active tuberculosis and 20 healthy individuals with a diverse representation of
215 polymorphisms, but the number of participants with G191A mutations was limited (n=5). A
216 larger validation study involving testing on whole blood, including from finger stick capillary
217 blood, is needed to assess real-world performance of this assay under field conditions. Further
218 studies should also investigate testing on non-invasive samples including saliva or oral swabs,
219 from which DNA is abundant. Second, we focused on NAT2 polymorphisms, as they explain
220 88% of interindividual pharmacokinetic variability, though polymorphisms in several other
221 genes have been associated with hepatotoxicity. However, these associations have been
222 comparatively modest and somewhat inconsistent³⁶⁻⁴⁰. We focused on isoniazid and did not
223 include other important tuberculosis drugs, such as rifampicin. The evidence base for
224 pharmacogenomic markers predicting rifampin pharmacokinetics is less robust, and findings
225 concerning clinical outcomes such as toxicities or treatment response are limited^{41,42}. However,
226 given the importance of this drug class in treatment of active and latent tuberculosis, and
227 emerging evidence supporting greater efficacy of higher doses of rifampin, further investigation
228 of pharmacogenomic markers in rifampicin is needed. Future assays may include polymorphisms
229 influencing rifampicin metabolism to further optimize treatment of tuberculosis.

230

231 Since the demonstration of the efficacy of six month, short-course chemotherapy in 1979,
232 standardized treatment for drug susceptible tuberculosis using weight-based doses has remained
233 essentially unchanged⁴³. Additionally, isoniazid remains a major component of regimens for
234 treatment of latent tuberculosis, which is recommended by the WHO for young children, HIV-
235 infected individuals and household contacts of tuberculosis cases⁴⁴. More than half the world's

236 population have slow or rapid acetylation phenotypes, which put them at risk for excessive drug
237 levels resulting in drug toxicities or insufficient drug levels putting them at risk of acquired drug
238 resistance or disease relapse. Dose adjustment based on NAT2 acetylation genotyping can
239 achieve consistent, target drug levels and reduce the incidence of poor clinical outcomes. We
240 developed a prototype automated, cartridge-based assay that can reliably predict acetylation
241 phenotype directly from as low as 25 ul of whole blood. By developing this for the GeneXpert
242 platform, which is widely used in low- and middle-income countries for tuberculosis diagnosis,
243 this assay could make personalized tuberculosis treatment dosing available in resource-
244 constrained settings. Further studies are needed to evaluate its accuracy and clinical impact in
245 real-world clinical settings.

246

247 **METHODS**

248

249 **Ethics statement**

250 The clinical study was approved by the institutional review boards of the Stanford University
251 School of Medicine and Federal University of Grande Dourados (IRB#33005). All participants
252 were over the age of 18 and provided written informed consent. For assay optimization and
253 validation on GeneXpert cartridge, anonymized blood samples from healthy individuals were
254 obtained from Stanford blood center.

255

256 **Datasets**

257 The datasets used to develop the NAT2 classifier was obtained from the IGSR (International
258 Genome Sample Resource, 1000 genomes project) and a meta-analysis by Sabbagh et. al^{4,25}.
259 Population information on the combined dataset is provided in **Supplementary Table 3**.

260 **NAT2 acetylator phenotype prediction classifier**

261 Phased genomes from 8,561 individuals were used and haplotypes were labeled based on 7
262 polymorphic sites in the *NAT2* gene (191G>A, 282C>T, 341T>C, 481C>T, 590G>A, 803A>G
263 and 857G>A), following an international consensus nomenclature (43). Individuals with two
264 slow haplotypes were considered slow acetylators; those with two rapid haplotypes were
265 considered rapid acetylators; and those with one slow and one rapid acetylator were considered
266 intermediate acetylators. We then constructed an unphased dataset containing only information
267 on whether each sample was wild type for both alleles, homozygous variant for both alleles, or
268 heterozygous. We then split the dataset into two-thirds for a training set and one third for an out-
269 of-sample test set, using sampling stratified by geographic representation to ensure
270 representativeness in the training and test sets. We trained a random forest model on the training
271 set using the *caret* package in R⁴⁵ and assessed classification performance on the test set. We
272 began with a 7 SNP model and eliminated SNPs in sequential models according to the lowest
273 variable importance factor.

274

275 **Sample collection**

276 Sputum and plasma samples from 49 newly diagnosed patients with active pulmonary
277 tuberculosis were collected at the Federal University of Grande Dourados, Brazil. All
278 participants were treated with standardized, weight-based doses of isoniazid, rifampicin,

279 pyrazinamide and ethambutol. Plasma samples were collected at 1 hour and 8 hours after the first
280 dose and after 1 hour on day 14. Plasma drug concentrations for isoniazid and acetyl-isoniazid
281 were quantified by high-performance liquid chromatography coupled to tandem mass
282 spectrometry (HPLC-MS) as previously described.⁴⁶

283

284 **Reference NAT2 SNP genotyping assays**

285 *Sputum processing, host DNA extraction and single-plex assays on clinical samples*

286 Spontaneously expectorated sputum from confirmed pulmonary tuberculosis patients was
287 collected in approximately 10mL of guanidine thiocyanate (GTC) solution (5 M guanidinium
288 thiocyanate, 0.5% w/v sodium N-lauryl sarcosine, 25 mM trisodium citrate, 0.1 M 2-
289 mercaptoethanol, 0.5% w/v Tween 80 [pH 7.0]) as described previously⁴⁷. The samples were
290 needle sheared and centrifuged at 3000 rpm for 30 min. The supernatant was removed leaving
291 behind 1ml pellet. The pellet was centrifuged at 11,500 rpm for 3 min. Approximately 0.5 ml
292 supernatant was transferred to a fresh cryovial and 0.75 ml Trizol LS was added to the
293 supernatant. The samples were frozen at -80 until used. Host DNA was extracted from the
294 supernatant using a manual extraction method described previously⁴⁸. The DNA was eluted in 50
295 ul DNase-free water and quantified on Qubit. Approximately 10 ng of genomic DNA was used
296 for each single-plex melt curve and commercial TaqMan SNP (NAT2 TaqMan® SNP
297 Genotyping Assays, Applied Biosystems) assay.

298

299 *DNA extraction from whole blood samples from healthy individuals*

300 For 5-plex assay validation, genomic DNA from 100ul of whole blood from healthy individuals
301 was extracted using Qiagen Blood and tissue kit (# 69504). The DNA was eluted in 30ul DNase-
302 free water and quantified on Qubit. 100ng of DNA was used for Sanger sequencing validation.

303

304 **PCR amplification for Sanger DNA sequencing**

305 For DNA sequencing, an 823 bp fragment of the NAT2 gene (819–1641 bp of the gene) was
306 amplified using the forward primer 5'-GGGCTGTTCCCTTTGAGA-3' and reverse primer 5'-
307 TAGTGAGTTGGGTGATAC-3'. A 20 µl PCR mixture contained 0.5 µl of each forward and
308 reverse primers from 10 µM stocks, 8 µl double distilled water, 0.5ul Phusion Taq polymerase
309 and 1 µl (~100ng) DNA template. PCR was performed with initial denaturation at 95°C for 5
310 min followed by 30 cycles of denaturation at 95°C for 30 s, annealing at 55°C for 30 s and
311 extension at 72°C for 1 min, with an additional extension at 72°C for 10 min. PCR products were
312 analyzed on 1.5% agarose gels to confirm size of product which was then sequenced at the
313 (Stanford PAN Facility, CA).

314

315 **Primers and probes for melt curve analysis**

316 Three sets of primers spanning the *NAT2* gene were used for single-plex and multiplex PCR.
317 Primers and sloppy molecular beacon (SMB) probes were designed using Beacon Designer
318 (Premier Biosoft International, Palo, CA; version 8). Three of 5 molecular beacon probes
319 (NAT2-191, NAT2-590 and NAT2-857) were designed with 100% complementarity towards
320 mutant alleles and two (NAT2-282 and NAT2-341) were 100% specific to wild type alleles. For
321 single-plex assays, all probes were labelled with FAM at their 5' end and BHQ-1 at 3'. For the
322 multiplex assay on GeneXpert, FAM was replaced with other fluorophores except for NAT2-

323 590. A list of primers and probes sequences for the multiplex assay with their corresponding
324 fluorophores and quenchers is provided in **Supplementary Table 4**.

325

326 **Single-plex PCR and melt curve analysis on pulmonary TB patients**

327 Genomic DNA extracted from sputum samples from TB positive patients was used for single-
328 plex assays performed on StepOne Plus Real Time PCR. A 20ul total reaction volume was set up
329 using 10ng genomic DNA per assay. PCR mastermix included (0.5 ul of 2U Aptataq exo-DNA
330 polymerase, 1X betaine, 1X Aptataq buffer, 4mM MgCl₂, 1X ROX passive reference dye, 60nM
331 FP,1000nM reverse primers, 250uM of each probe). PCR was initiated by 10 min of
332 denaturation–activation at 95°C, followed by 50 cycles at 95°C for 15 sec (denaturation),
333 annealing at 60°C for 15 s and extension at 76°C for 20sec. The melting program included three
334 steps: denaturation at 95°C for 1 min, followed by renaturation at 35°C for 3 min and a
335 continuous reading of fluorescence from 45 to 85°C by heating at increments of 0.03°C/s. The
336 MMCA curve was analyzed using the StepOne Plus software version 2.0. For single-plex melt
337 curve assay validation, TaqMan 7-SNP genotyping assays were performed using commercial
338 assays (NAT2 TaqMan® SNP Genotyping Assays, Applied Biosystems) on DNA extracted from
339 sputum samples from 49 pulmonary TB patients on a StepOne Plus Real Time PCR machine.

340

341 **Pharmacokinetic analysis of INH clearance in tuberculosis patients**

342 The population PK analysis was performed using the non-linear mixed effects modeling
343 approach using NONMEM (version 7.4.3; ICON plc, Gaithersburg, MD, USA), PsN and R-
344 based Xpose (version 4.7 and higher)^{49,50}. One-compartment model with a first-order absorption
345 with a lognormal distribution for inter-individual variability (IIV) on different PK parameter(s)

346 as well as an additive and/or proportional model for the residual error were tested for the base
347 model selection. Mixture models with two or three subpopulations representing different
348 clearance rate were then evaluated. The first-order conditional estimation with interaction
349 method (FOCEI) was applied and the model-building procedure and model selection was based
350 on the log-likelihood criterion (the difference in the minimum OFV between hierarchical models
351 was assumed to be Chi-square distributed with degrees of freedom equal to the difference in the
352 number of parameters between models), goodness-of-fit plots (e.g. relevant residuals against
353 time randomly distributed around zero), and scientific plausibility of the model. Visual predictive
354 check was conducted to evaluate whether the final model with estimated fixed-effect parameters
355 and covariates adequately describe data.

356

357 **Automated NAT2-PGx Multiplex PCR and melt curve analysis**

358 Asymmetric PCR and melt curve analysis were performed on a GeneXpert IV instrument using
359 GeneXpert Dx 4.8 software (Cepheid, Sunnyvale). Flex cartridge-01 (Cepheid) were used to
360 perform automated DNA extraction from whole blood followed by PCR amplification and melt
361 curve analysis to detect SNPs. PCR and melt conditions were optimized using mastermix
362 prepared in house. The NAT2-PGx assay was performed in an 80ul reaction volume (70ul
363 mastermix and 10ul eluted DNA). Briefly, 100ul of whole blood was mixed with 900ul of lysis
364 buffer (Cepheid) in a 1.5ml Eppendorf tube. The sample was vortexed for 2-3 sec and incubated
365 at room temperature for 2min. The entire 1ml whole blood and lysis buffer mix was loaded into
366 sample preparation chamber of flex cart-01 for automated DNA extraction. 70ul PCR mastermix
367 was simultaneously loaded in the PCR reaction chamber of the flex cart-01. The GeneXpert was
368 programmed to elute DNA in 10ul volume which was used for the NAT2-PGx assay. PCR

369 mastermix included (2ul of 2U Aptataq exo-DNA polymerase, 1X Betaine, 1X PCR additive
370 reagent, 1X Aptataq buffer, 8mM MgCl₂, 400nM FP, 900nM reverse primers, 500nM of 191-
371 Cy5.5 and 857-Alexa-405, 430nM 282-Alexa-647 and 590-FAM and 300nM 341-Alexa-537
372 probes). PCR was initiated at holding stage- 50°C for 2min, initial denaturation at 94°C for
373 2min, followed by 50 cycles of denaturation at 95°C for 15 sec, annealing at 57°C for 30 sec and
374 extension at 65°C for 60 sec. The melting program included three steps: denaturation at 95°C for
375 1 min, followed by renaturation at 40°C for 3 min and a continuous reading of fluorescence from
376 40 to 72°C by heating at increments of 0.05°C/sec. The MMCA curve was analyzed using the
377 GXP version 4.8 software.

378
379 We validated the automated NAT2-PGx assay by analyzing 20 blood samples, for which
380 polymorphisms in the 5 positions were confirmed by Sanger sequencing. We assessed analytical
381 sensitivity of the assay and robustness to input blood volume by performing it on varying
382 volumes of whole blood (200 ul, 100 ul, 50 ul, 25 ul) and comparing the T_m results and standard
383 deviation for each position across blood volumes.

384
385 **Funding**

386
387 FleXcartridges and technical support for their use were provided by Cepheid. This study was
388 supported by the Institute for Immunity, Transplantation, and Infection and the Department of
389 Medicine at Stanford University.

390
391 **Reporting summary.** Further information on research design is available in the Nature Research
392 Reporting Summary linked to this article.

393

394 **Data availability**

395 Data supporting the findings of this manuscript are available in the Supplementary Information
396 files or from the corresponding author upon request.

397

398 **Code availability**

399

400 Code and dataset used to develop NAT2 classifier are provided with the manuscript.

401

402 **Acknowledgements**

403 We thank Veronique Dartois for performing the plasma drug level assays.

404

405 **Author contributions**

406 JRA and RV conceived of the study. RV, JC, and JRA designed the experiments. RV, SP,

407 FMM, MTV, ASS and JC collected data. RV, NZ, RS and JRA analyzed data. EW, DG and DP

408 provided technical guidance on the assay development. RV and JRA wrote the first draft of the

409 manuscript, and all authors contributed to the final version.

410 **Conflicts of Interest**

411 JRA and RV are named co-inventors on a provisional patent (Application number 62/991,477) for

412 a *NAT2* pharmacogenomic assay.

413 **References**

- 414 1. Gillespie SH. et al. Consortium. Four-month moxifloxacin-based regimens for drug-
415 sensitive tuberculosis. *N Engl J Med.* 2014 Oct 23;371(17):1577-87.
- 416 2. Merle CS. et al. OFLOTUB/Gatifloxacin for Tuberculosis Project. A four-month
417 gatifloxacin-containing regimen for treating tuberculosis. *N Engl J Med.* 2014 Oct
418 23;371(17):1588-98.
- 419 3. Jindani A. et al. High-dose rifapentine with moxifloxacin for pulmonary tuberculosis. *N*
420 *Engl J Med.* 2014 Oct 23;371(17):1599-608.
- 421 4. Pratt VM. et al. Characterization of 137 Genomic DNA Reference Materials for 28
422 Pharmacogenetic Genes: A GeT-RM Collaborative Project. *J Mol Diagn.* 2016
423 Jan;18(1):109-23.
- 424 5. García-Martín E. Interethnic and intraethnic variability of NAT2 single nucleotide
425 polymorphisms. *Curr Drug Metab.* 2008 Jul;9(6):487-97.
- 426 6. Schaberg T et al. Risk factors for side-effects of isoniazid, rifampin and pyrazinamide in
427 patients hospitalized for pulmonary tuberculosis. *Eur Respir J.* 1996 Oct;9(10):2026-30.
- 428 7. Saukkonen JJ. et al. Hepatotoxicity of Antituberculosis Therapy Subcommittee. An
429 official ATS statement: hepatotoxicity of antituberculosis therapy. *Am J Respir Crit Care*
430 *Med.* 2006 Oct 15;174(8):935-52.
- 431 8. Schutz C. et al. Burden of antituberculosis and antiretroviral drug-induced liver injury at
432 a secondary hospital in South Africa. *S Afr Med J.* 2012 Mar 2;102(6):506-11.
- 433 9. Luzze H. et al. Relapse more common than reinfection in recurrent tuberculosis 1-2 years
434 post treatment in urban Uganda. *Int J Tuberc Lung Dis.* 2013 Mar;17(3):361-7

- 435 10. Romanowski K. et al. Predicting tuberculosis relapse in patients treated with the standard
436 6-month regimen: an individual patient data meta-analysis. *Thorax*. 2019 Mar;74(3):291-
437 297.
- 438 11. Pasipanodya JG. et al. Meta-analysis of clinical studies supports the pharmacokinetic
439 variability hypothesis for acquired drug resistance and failure of antituberculosis therapy.
440 *Clin Infect Dis*. 2012 Jul;55(2):169-77.
- 441 12. Gumbo T. et al. Isoniazid bactericidal activity and resistance emergence: integrating
442 pharmacodynamics and pharmacogenomics to predict efficacy in different ethnic
443 populations. *Antimicrob Agents Chemother*. 2007 Jul;51(7):2329-36.
- 444 13. Pasipanodya JG. et al. Serum drug concentrations predictive of pulmonary tuberculosis
445 outcomes. *J Infect Dis*. 2013 Nov 1;208(9):1464-73.
- 446 14. Kinzig-Schippers M, Tomalik-Scharte D, Jetter A, Scheidel B, Jakob V, Rodamer M,
447 Cascorbi I, Doroshenko O, Sörgel F, Fuhr U. Should we use N-acetyltransferase type 2
448 genotyping to personalize isoniazid doses? *Antimicrob Agents Chemother*. 2005
449 May;49(5):1733-8.
- 450 15. Sabbagh A. et al. Worldwide distribution of NAT2 diversity: implications for NAT2
451 evolutionary history. *BMC Genet*. 2008 Feb 27;9:21.
- 452 16. Wang PY. et al. NAT2 polymorphisms and susceptibility to anti-tuberculosis drug-
453 induced liver injury: a meta-analysis. *Int J Tuberc Lung Dis*. 2012 May;16(5):589-95.
- 454 17. Du H. et al. Slow N-acetyltransferase 2 genotype contributes to anti-tuberculosis drug-
455 induced hepatotoxicity: a meta-analysis. *Mol Biol Rep*. 2013 May;40(5):3591-6.
- 456 18. Azuma J. et al. Pharmacogenetics-based tuberculosis therapy research group. NAT2
457 genotype guided regimen reduces isoniazid-induced liver injury and early treatment

- 458 failure in the 6-month four-drug standard treatment of tuberculosis: a randomized
459 controlled trial for pharmacogenetics-based therapy. *Eur J Clin Pharmacol.* 2013
460 May;69(5):1091-101.
- 461 19. Snider DE Jr. et al. Isoniazid-associated hepatitis deaths: a review of available
462 information. *Am Rev Respir Dis.* 1992 Feb;145(2 Pt 1):494-7.
- 463 20. Kuznetsov IB. et al. A web server for inferring the human N-acetyltransferase-2 (NAT2)
464 enzymatic phenotype from NAT2 genotype. *Bioinformatics.* 2009 May 1;25(9):1185-6.
- 465 21. Ramachandran G. et al. Role of pharmacogenomics in the treatment of tuberculosis: a
466 review. *Pharmgenomics Pers Med.* 2012;5:89-98.
- 467 22. McInnes G. et al. Drug Response Pharmacogenetics for 200,000 UK Biobank
468 Participants. doi: <https://doi.org/10.1101/2020.08.09.243311>
- 469 23. Rens NE. et al. Cost-Effectiveness of a Pharmacogenomic Test for Stratified Isoniazid
470 Dosing in Treatment of Active Tuberculosis. *Clin Infect Dis.* 2020 Jan 6:ciz1212.
- 471 24. Sabbagh A. et al. Evaluating NAT2PRED for inferring the individual acetylation status
472 from unphased genotype data. *BMC Med Genet.* 2009 Dec 31;10:148.
- 473 25. Sabbagh A. et al. Arylamine N-acetyltransferase 2 (NAT2) genetic diversity and
474 traditional subsistence: a worldwide population survey. *PLoS One.* 2011 Apr
475 6;6(4):e18507.
- 476 26. Van Oosterhout JJ. et al. Pharmacokinetics of Antituberculosis Drugs in HIV-Positive
477 and HIV-Negative Adults in Malawi. *Antimicrob Agents Chemother.* 2015
478 Oct;59(10):6175-80.
- 479 27. Wilkins JJ. et al. Variability in the population pharmacokinetics of isoniazid in South
480 African tuberculosis patients. *Br J Clin Pharmacol.* 2011 Jul;72(1):51-62.

- 481 28. Wilkins JJ. et al. Population pharmacokinetics of rifampin in pulmonary tuberculosis
482 patients, including a semimechanistic model to describe variable absorption. *Antimicrob*
483 *Agents Chemother.* 2008 Jun;52(6):2138-48.
- 484 29. Wilkins JJ. et al. Variability in the population pharmacokinetics of pyrazinamide in South
485 African tuberculosis patients. *Eur J Clin Pharmacol.* 2006 Sep;62(9):727-35.
- 486 30. Iselius L. et al. Formal genetics of isoniazid metabolism in man. *Clin Pharmacokinet.*
487 1983 Nov-Dec;8(6):541-4.
- 488 31. Evans DA. Genetic variations in the acetylation of isoniazid and other drugs. *Ann N Y*
489 *Acad Sci.* 1968 Jul 31;151(2):723-33.
- 490 32. Evans DA. An improved and simplified method of detecting the acetylator phenotype. *J*
491 *Med Genet.* 1969 Dec;6(4):405-7.
- 492 33. Donald PR. et al. The influence of dose and N-acetyltransferase-2 (NAT2) genotype and
493 phenotype on the pharmacokinetics and pharmacodynamics of isoniazid. *Eur J Clin*
494 *Pharmacol.* 2007 Jul;63(7):633-9.
- 495 34. Lee SW. et al. NAT2 and CYP2E1 polymorphisms and susceptibility to first-line anti-
496 tuberculosis drug-induced hepatitis. *Int J Tuberc Lung Dis.* 2010 May;14(5):622-6.
- 497 35. Roy B. et al. Predisposition of antituberculosis drug induced hepatotoxicity by
498 cytochrome P450 2E1 genotype and haplotype in pediatric patients. *J Gastroenterol*
499 *Hepatol.* 2006 Apr;21(4):784-6.
- 500 36. Simon T. et al. Combined glutathione-S-transferase M1 and T1 genetic polymorphism
501 and tacrine hepatotoxicity. *Clin Pharmacol Ther.* 2000 Apr;67(4):432-7.
- 502 37. Strange RC. et al. Glutathione S-transferase: genetics and role in toxicology. *Toxicol*
503 *Lett.* 2000 Mar 15;112-113:357-63.

- 504 38. Ramachandran G. et al. Role of pharmacogenomics in the treatment of tuberculosis: a
505 review. *Pharmacogenomics Pers Med.* 2012;5:89-98.
- 506 39. Mukonzo JK. et al. Role of pharmacogenetics in rifampicin pharmacokinetics and the
507 potential effect on TB-rifampicin sensitivity among Ugandan patients. *Trans R Soc Trop*
508 *Med Hyg.* 2020 Feb 7;114(2):107-114.
- 509 40. Naidoo A. et al. Effects of genetic variability on rifampicin and isoniazid
510 pharmacokinetics in South African patients with recurrent tuberculosis.
511 *Pharmacogenomics.* 2019 Mar;20(4):225-240.
- 512 41. Medellin-Garibay SE. et al. A population approach of rifampicin pharmacogenetics and
513 pharmacokinetics in Mexican patients with tuberculosis. *Tuberculosis (Edinb).* 2020
514 Sep;124:101982.
- 515 42. *Database of arylamine N-acetyltransferases* (<http://nat.mbg.duth.gr>)
- 516 43. Clinical trial of six-month and four-month regimens of chemotherapy in the treatment of
517 pulmonary tuberculosis. *Am Rev Respir Dis.* 1979 Apr;119(4):579-85.
- 518 44. Haley CA. Treatment of Latent Tuberculosis Infection. *Microbiol Spectr.* 2017 Apr;5(2).
- 519 45. Kuhn M. et al. (2019). caret: Classification and Regression Training. R package version
520 6.0-84. <https://CRAN.R-project.org/package=caret>
- 521 46. Prideaux B. et al. The association between sterilizing activity and drug distribution into
522 tuberculosis lesions. *Nat Med.* 2015 Oct;21(10):1223
- 523 47. Walter ND. et al. Transcriptional Adaptation of Drug-tolerant Mycobacterium
524 tuberculosis During Treatment of Human Tuberculosis. *J Infect Dis.* 2015 Sep
525 15;212(6):990-8.

- 526 48. Chomczynski P. A reagent for the single-step simultaneous isolation of RNA, DNA and
527 proteins from cell and tissue samples. *Biotechniques*. 1993 Sep;15(3):532-4, 536-7.
- 528 49. Beal SL. Et al. NONMEM 7.4 Users Guides. (1989– 2019). ICON plc, Gaithersburg,
529 MD. <https://nonmem.iconplc.com/nonmem744>
- 530 50. Lindbom L. et al. (2004). Perl-speaks-NONMEM (PsN)--a Perl module for NONMEM
531 related programming. *Comput Methods Programs Biomed*, 75 (2), 85-94.
- 532
- 533
- 534
- 535

536 **Figure 1. Predicted NAT2 phenotype from sputum samples and associated acetylation ratio**
537 **and isoniazid clearance rates from patients receiving tuberculosis treatment.** The (a) 8 hour
538 acetyl-INH to INH ratio and (b) isoniazid clearance rates, according to acetylation phenotype
539 predicted from 5 SNPs, measured in sputum samples from 49 patients receiving treatment for
540 active tuberculosis.

541
542 **Figure 2. Schemata for the automated NAT2 Pharmacogenomic assay.** 1-2 drops of blood is
543 collected in an Eppendorf tube and mixed with lysis buffer to a total of 1 ml, which is then
544 loaded onto a GeneXpert Flex01 cartridge and placed into a GeneXpert instrument for automated
545 DNA extraction, asymmetric PCR and meltcurve analysis. Allele patterns for each of the 5 SNPs
546 are determined by Tm analysis, and the resulting data are used to predict acetylator phenotype.

547
548 **Figure 3. Negative derivative transformed melt curves for the five NAT2 gene**
549 **polymorphisms.** The shift in melt curve temperature is observed during a nucleotide exchange.
550 Sloppy molecular beacon probes are first hybridized and then melted off of their NAT2 target
551 amplicon. The melt curves indicate wild type alleles at positions 191(red), 341(green) and 857
552 (orange); and mutant alleles at positions 282(Blue) and 590(Purple).

553
554 **Figure 4. Effect of whole blood sample volume on melting temperature for wild type and**
555 **mutant alleles at 5 positions in NAT2:** NAT2 polymorphisms were accurately detected at all
556 volumes with sufficient different in melting temperature (Tm) to distinguish wild type from
557 mutant alleles. No individuals in this dataset had mutations at position 191.

558

559 **Table 1. Summary of populations included in genomic analysis and their acetylation**
560 **genotypes.**

561

Region	Number of individuals	Acetylation Genotype, n (%)		
		Slow	Intermediate	Rapid
Americas	1,112	432 (39%)	463 (42%)	217 (20%)
Central and South Asia	588	355 (60%)	198 (34%)	35 (6%)
East Asia	2,308	340 (15%)	1049 (45%)	919 (40%)
Europe	3,458	1966 (57%)	1249 (36%)	243 (7%)
North Africa	44	30 (68%)	10 (23%)	4 (9%)
sub-Saharan Africa	1,051	450 (43%)	459 (44%)	142 (14%)
Total	8,561	3573 (42%)	3428 (40%)	1560 (18%)

562

563

564 **Table 2. Out-of-sample prediction accuracy of unphased NAT2 SNP data for acetylation**

565 **phenotype in random forest models.** Models were trained with 5,738 individuals and tested on

566 2,823 individuals. Sens: sensitivity. Spec: specificity.

567

NAT2 SNP Positions	SNP number	Accuracy	95% CI	Sens. Rapid	Spec. Rapid	Sens. Slow	Spec Slow
191, 282, 341, 481, 590, 803, 857	7	1.000	(0.999-1.000)	1.000	1.000	1.000	1.000
191, 282, 341, 481, 590, 857	6	1.000	(0.999-1.000)	1.000	1.000	1.000	1.000
191, 282, 341, 590, 857	5	1.000	(0.999-1.000)	1.000	1.000	1.000	1.000
282, 341, 590, 857	4	0.978	(0.972-0.983)	0.996	0.988	0.969	0.999
341, 590, 847	3	0.976	(0.970-0.982)	1.000	0.986	0.967	1.000
341, 590	2	0.852	(0.838-0.865)	1.000	0.889	0.832	1.000

568

569

570

571

572

573

574

575 **Table 3. Melting temperature (T_m) values for five NAT2 polymorphisms derived from**
 576 **DNA-probe hybrid melts using single-plex assays validated on 49 pulmonary TB patients**
 577

	Mutant	Wild type	Het	Mutant	Wild type	
NAT2 SNP position	Total samples analyzed	Total samples analyzed	Total samples analyzed	T _m ± SD	T _m ± SD	ΔT _m (WT-MT)
191	0	44	5	66.3 ± 0.28	61.92 ± 0.68	4.38
282	6	24	19	62.81 ± 0.40	66.85 ± 0.34	4.04
341	12	23	14	66.30± 0.48	68.70 ± 0.38	2.40
590	0	35	14	68.0 ± 0.28	64.37 ± 0.28	3.63
857	1	41	7	66.4± 0.11	62.72 ± 0.29	3.68

578 SD: Standard deviation

579

580

581 **Supplementary Table 1.** *NAT2* polymorphism profiles of 49 pulmonary TB patients detected
582 from 5-SNP and 7-SNP genotyping assays. Acetylator phenotypes predicted from 5-SNP, 6-SNP
583 and 7-SNP classifiers and plasma INH and acetyl-INH levels recorded at various time-points.

584

585 **Supplementary Table 2.** (a) *NAT2* genotype of whole blood samples (n=20) analyzed on 5-
586 plex *NAT2*-PGx assay and validated on Sanger sequencing. (b) *NAT2* genotypes of ten whole
587 blood samples analyzed using 200ul, 100ul, 50ul and 25ul samples

588

589 **Supplementary Table 3.** Population information on the dataset used to develop 5-SNP
590 classifier.

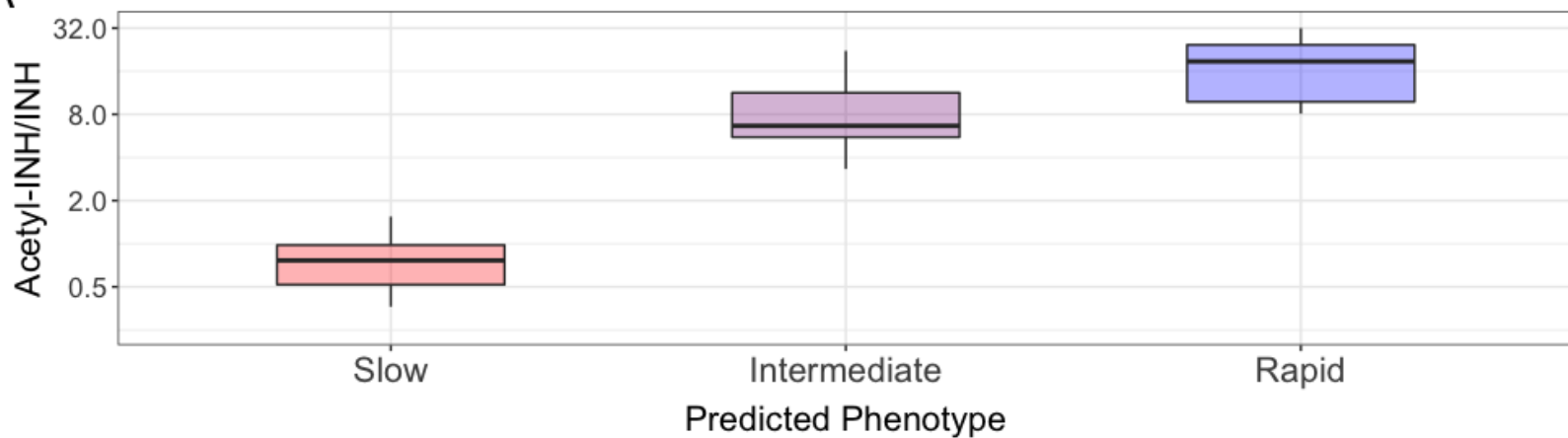
591

592 **Supplementary Table 4.** List of primers and probes sequences for multiplex assay with their
593 corresponding fluorophores and quenchers

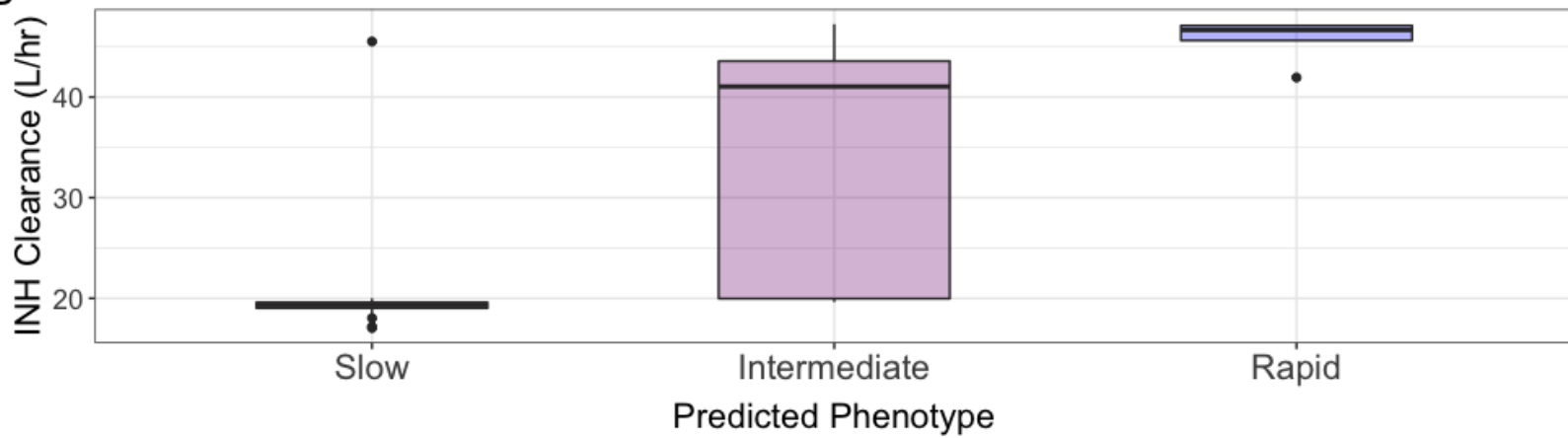
594

595

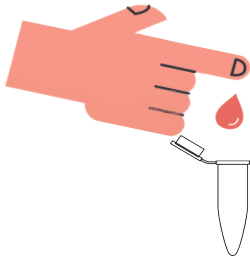
A



B

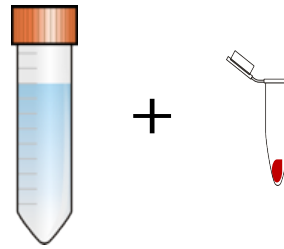


1 Sample collection



Collect 1-2 drops of whole blood (approx. 50ul)

2 Whole blood pretreatment



Mix 950ul lysis buffer, vortex for 2 sec and incubate at RT for 2min

3 Flex cart01 preparation



Pipette 1ml pretreated sample and 70ul PCR mastermix into the cartridge

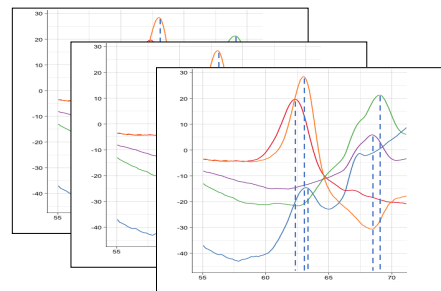
4 Automated DNA extraction & qPCR



Total run time= 140min

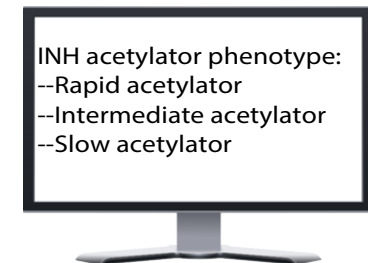
Load the cartridge in the GeneXpert machine and start the run

5 Data acquisition



Acquire melt curve data for NAT2 gene polymorphism detection

6 INH acetylator phenotype prediction



INH acetylator phenotype:
--Rapid acetylator
--Intermediate acetylator
--Slow acetylator

Upload NAT2 polymorphism data on phenotype prediction algorithm

